Supplementary Information

Mechanisms of Ni *N*-Heterocyclic Carbene Catalysts for C-O Bond Hydrogenolysis of Diphenyl Ether: A Density Functional Study

Boodsarin Sawatlon,[‡a] *Taveechai Wititsuwannakul,*[‡a] *Yuthana Tantirungrotechai,*[c] *and Panida Surawatanawong,*[*,a,b]

[a]Department of Chemistry and Center of Excellence for Innovation in Chemistry, Faculty of Science, Mahidol University, 272 Rama VI Road, Ratchathewi, Bangkok 10400, Thailand.

[b]Center for Alternative Energy, Mahidol University, 999 Phuttamonthon 4 Road, Salaya, Nakhon Pathom 73170, Thailand.

[c]Department of Chemistry, Faculty of Science, Thammasat University, Thailand

[‡]These authors contributed equally to this work.

*E-mail: panida.sur@mahidol.ac.th

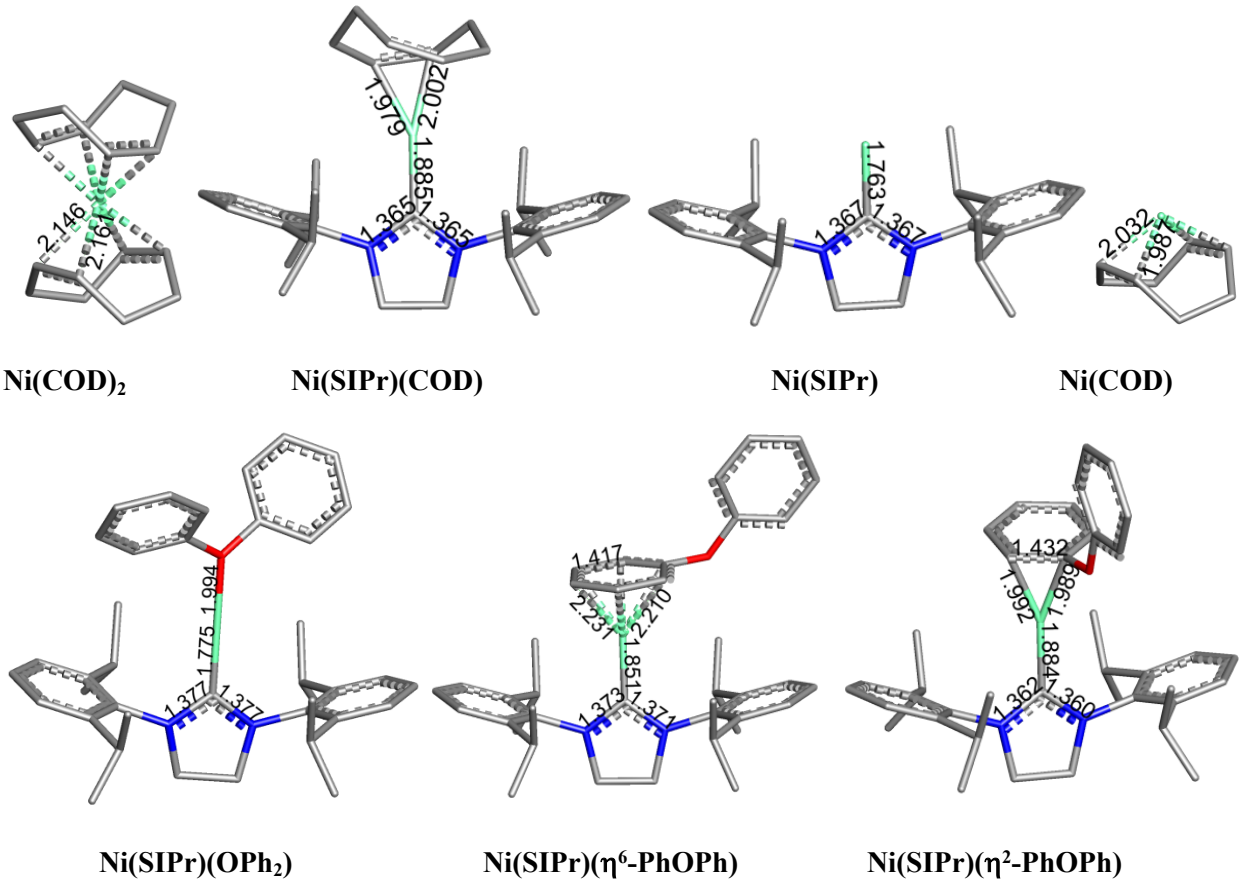

$Ni(COD)_2$ **Ni(SIPr)(COD)** **Ni(SIPr)** **Ni(COD)**

$Ni(SIPr)(OPh_2)$ **$Ni(SIPr)(\eta^6\text{-PhOPh})$** **$Ni(SIPr)(\eta^2\text{-PhOPh})$**

Fig. S1 Optimized structures in the formation of **Ni(SIPr)(η^2-PhOPh)** from the **$Ni(COD)_2$** precursor. All hydrogen atoms are omitted for clarity. Calculated bond distances are shown in Å. Ni atoms are shown in green, C atoms in grey, O atoms in red, and N atoms in blue.

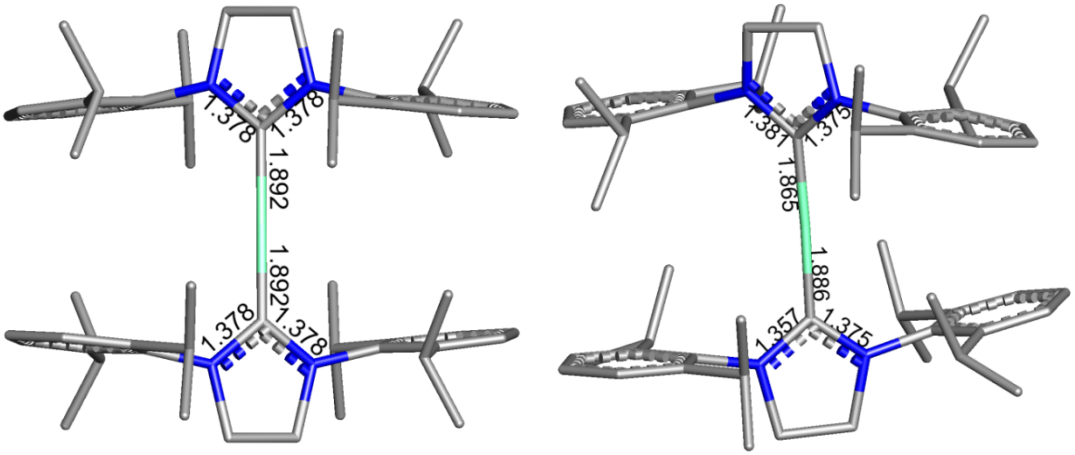

B3LYP/BS1 **X-Ray Crystal Structure[a]**

Fig. S2 Calculated structure and X-ray crystal structure[a] of $Ni(SIPr)_2$. Calculated bond distances are shown in Å. All hydrogen atoms are omitted for clarity.

[a]A. A. Danopoulos and D. Pugh, *Dalton Trans.*, 2008, 30-31.

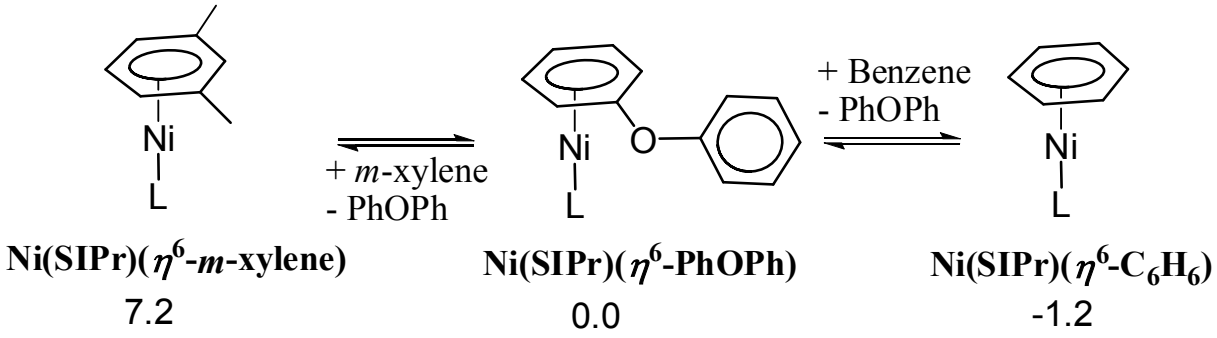

Fig. S3 Ligand substitution reaction of Ni(SIPr)(η^6-PhOPh). Solvent corrected free energies relative to Ni(SIPr)(η^6-PhOPh) in *m*-xylene are given in kcal/mol.

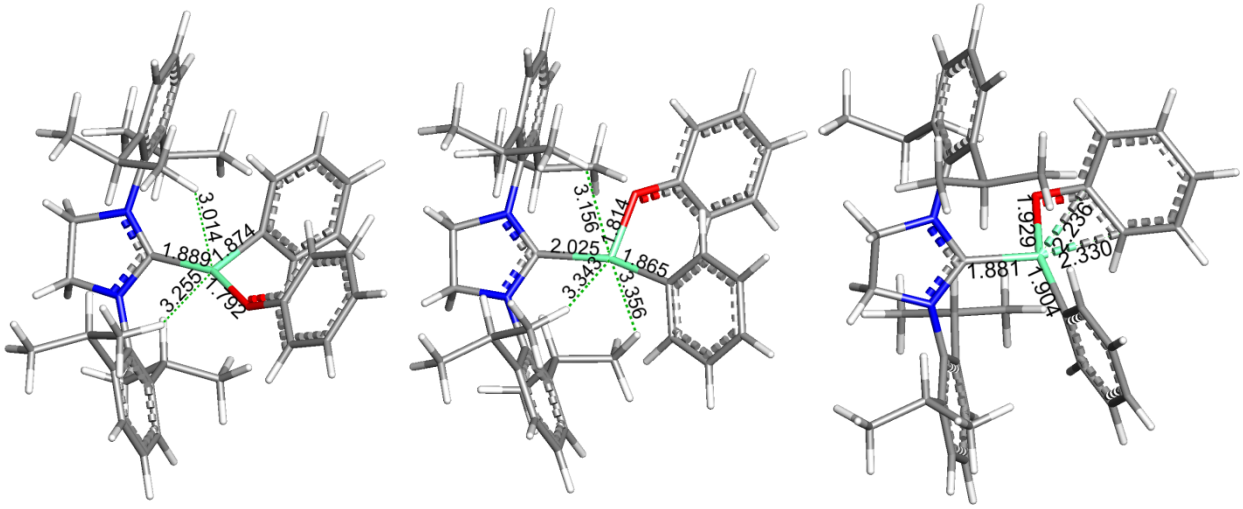

IN2 **IN3** **IN4**

Fig. S4 Optimized geometries of [Ni(SIPr)(Ph)(OPh)]^0: **IN2**, **IN3**, and **IN4**. Calculated bond distances are shown in Å.

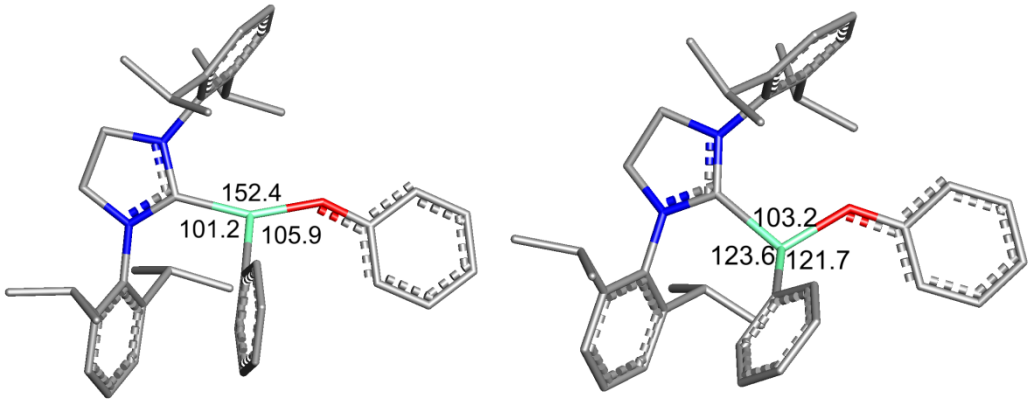

	IN2	**IN2$_T$**
Spin state	Singlet	Triplet
Relative free energy	0.0	2.8

Fig. S5 Optimized geometries of [Ni^{II}(SIPr)(Ph)(OPh)]^0 in the singlet (**IN2**) and in the triplet state (**IN2$_T$**). All H atoms are omitted for clarity. Selected bond angles are shown in degree (^{o}). Relative solvent corrected free energies in *m*-xylene are given in kcal/mol.

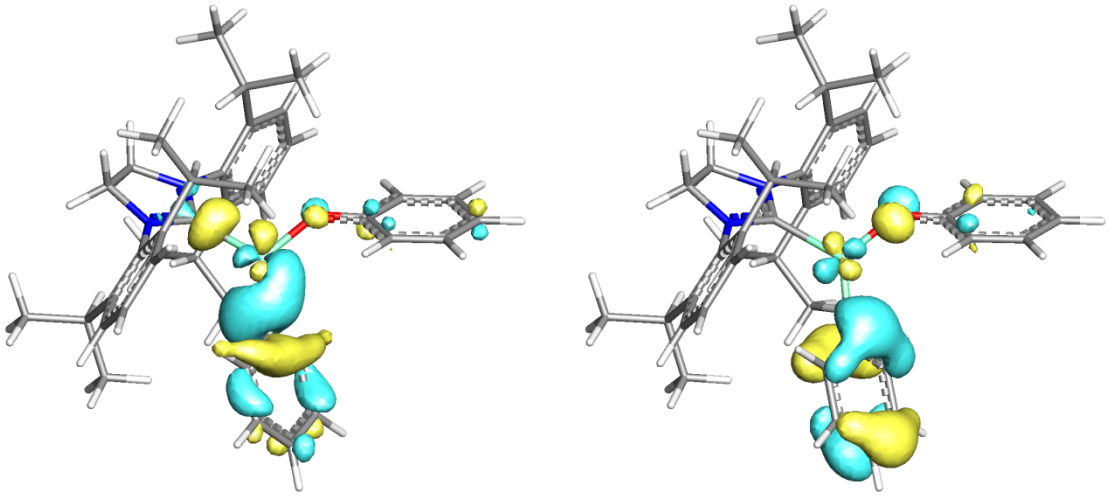

Ni d_{x2-y2}-based orbital Ni d_{xy}-based orbital

Fig. S6 Two singly occupied molecular orbitals (SOMOs) of **IN2$_T$**.

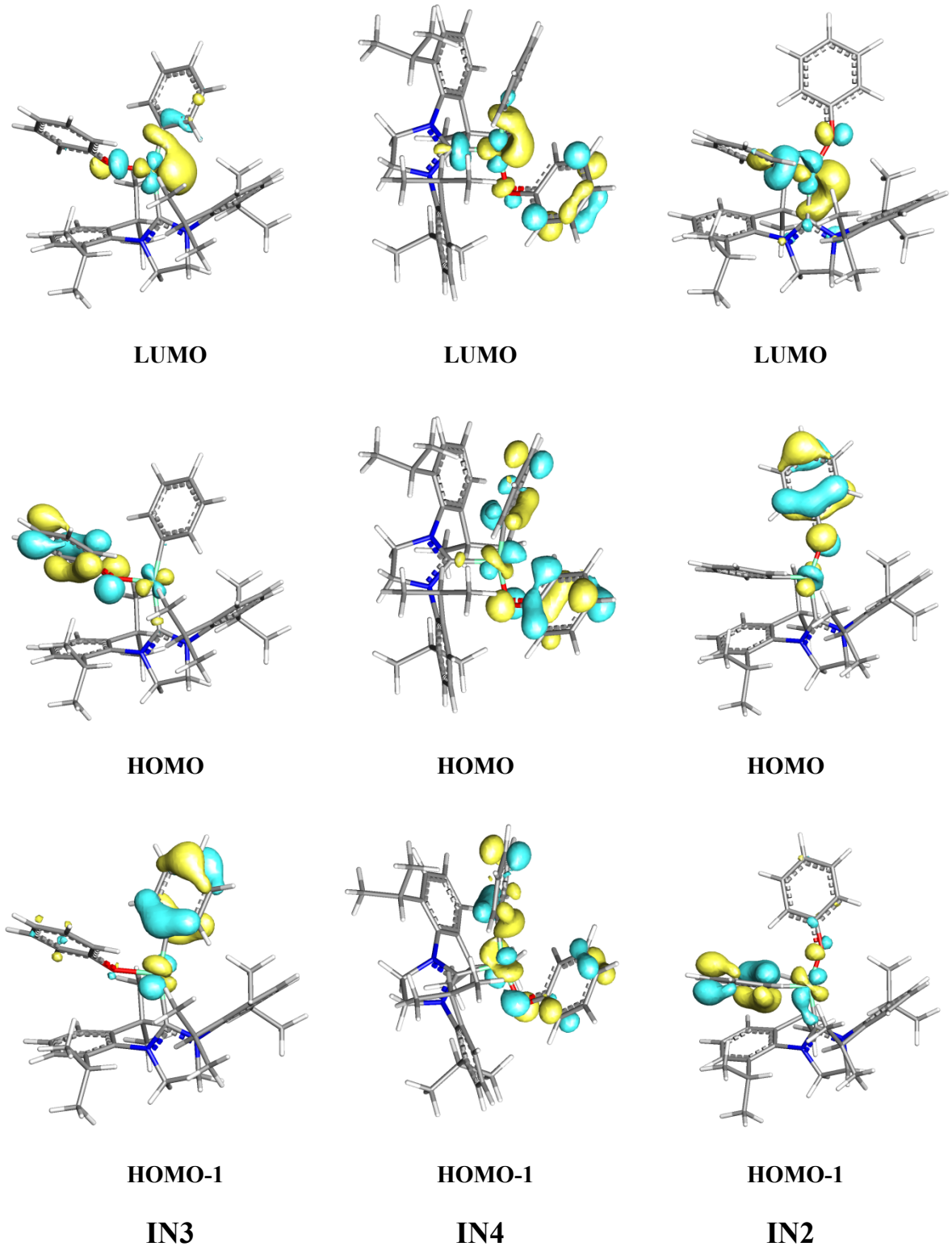

Fig. S7 Selected molecular orbitals of **IN3**, **IN4** and **IN2**.

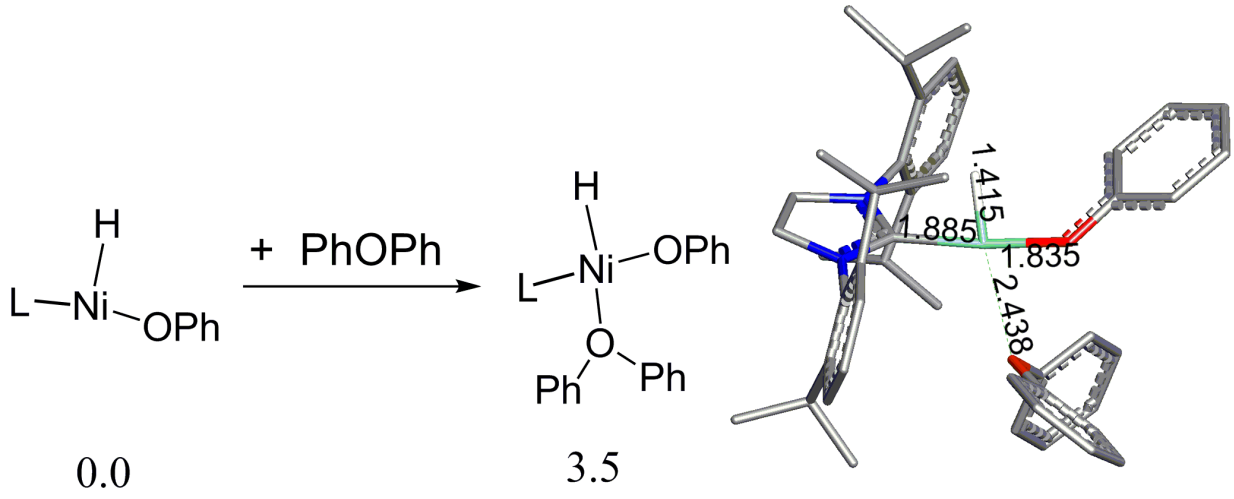

Fig. S8 Diphenyl ether coordination to Ni(SIPr)(H)(OPh) to form Ni(SIPr)(H)(OPh)(OPh_2). Relative solvent corrected free energies in *m*-xylene are given in kcal/mol. The optimized geometry of Ni(SIPr)(H)(OPh)(OPh_2) is presented and the selected bond distances are shown in Å.

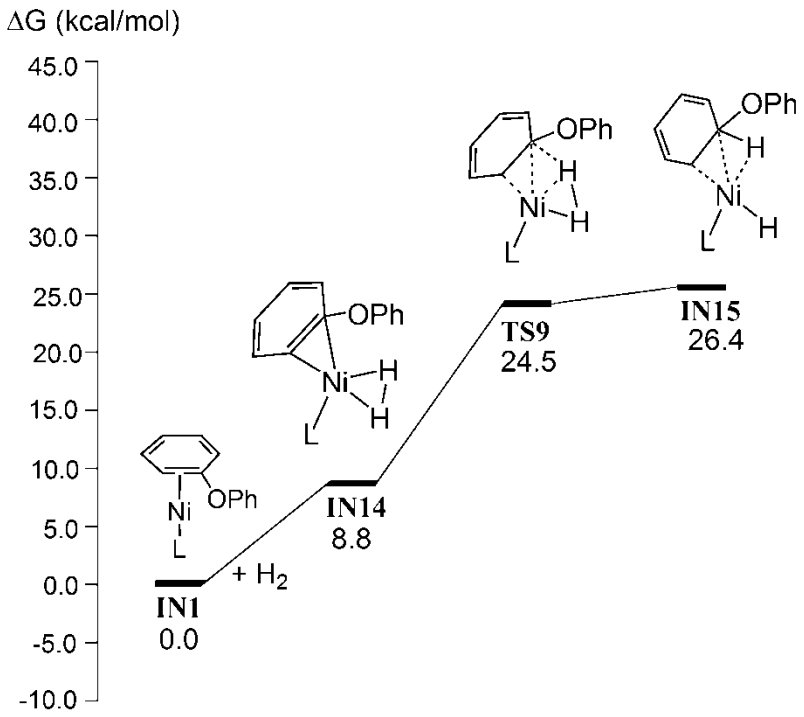

Fig. S9 Relative free energy profiles for the C-O bond hydrogenolysisof diphenyl ether *via* H_2 binding on **IN1**. Solvent corrected relative free energies in *m*-xylene are given in kcal/mol.

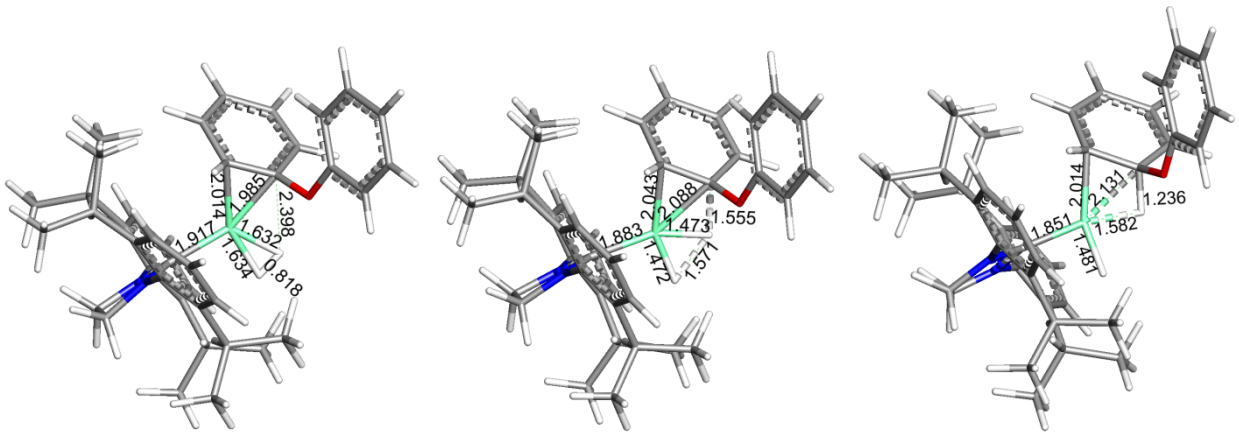

IN14 **TS9** **IN15**

Fig.S10 Optimized geometries of **IN14**, **TS9**, and **IN15**. Calculated bond distances are shown in Å.

Nickel Hydride Pathway

We calculated the binding of H_2 to **IN1** to form an H_2-complex Ni(SIPr)(η^2-PhOPh)(H_2), **IN14**, (Fig. S9). Generally, the dihydride mononuclear Ni complex is unstable[36], while the H_2 adducts of Ni complexes are observable and can undergo heterolytic cleavage assisted by an amine base.[37, 38] The nickel hydride pathway should involve *tert*-butoxide in abstracting a proton from **IN14** to generate the Ni-H species. Thus, the deprotonation of **IN14** by *tert*-butoxide base was investigated. However, sterical hindrance from the ligands around the Ni atom prevented *tert*-butoxide access to abstract the proton. To the best of our knowledge, currently there is no experimental support for the formation of nickel hydride intermediates under these reaction conditions. Therefore, we exclude the nickel hydride pathway in this study.

Alternatively, **IN14** can undergo H-transfer from Ni to the adjacent carbon of diphenyl ether *via* **TS9** (Fig. S9). **IN15** is subsequently formed, containing a CH agostic interaction with the Ni (Fig. S10). Although the energy barrier for H-transfer *via* **TS9** is relatively similar to that of the oxidative addition of PhOPh *via* **TS1** (24-26 kcal/mol), the transition state for the O-H bond formation process was not found. Moreover, analogous to **TS8** in the hydrogenation of benzene, the second H-transfer in **IN15** to form C_6H_7OPh is expected to proceed *via* a transition state with a high energy barrier. Therefore, the mechanism beyond **IN15** was not explored further.

Table S1. Relative electronic energies, enthalpies, gas-phase free energies, free energies with solvent correction at 1 atm, and free energies with solvent correction at 1 M (in kcal/mol) for C-O bond hydrogenolysis of diphenyl ether. The gas phase geometry structures were optimized by B3LYP/BS1. The solvent correction free energies were calculated by M06/BS2 in *m*-xylene.

	Relative Energy (kcal/mol)				
	B3LYP/BS1			M06/BS2	
	ΔE_{elec}	ΔH_{gas}	ΔG_{gas} (1atm)	ΔG_{sol} (1atm)	ΔG_{sol} (1M)
(a) The oxidative addition					
IN1 + PhOPh + H_2	0.0	0.0	0.0	0.0	0.0
TS1 + PhOPh + H_2	17.5	16.5	18.9	24.0	24.0
IN2 + PhOPh + H_2	-16.9	-16.5	-16.0	-5.2	-5.2
IN3 + PhOPh + H_2	-3.9	-3.9	-4.1	8.3	8.3
IN4 + PhOPh + H_2	-14.5	-14.2	-10.4	-6.8	-6.8
(b) The σ-Complex-Assisted Metathesis (σ-CAM)					
IN5 + PhOPh	-12.3	-9.6	1.4	2.5	0.7
TS2 + PhOPh	-0.9	0.3	11.5	16.0	14.1
IN7 + PhOPh	-12.5	-9.5	2.2	3.7	1.8
TS4 + PhOPh	0.9	2.2	14.3	17.0	15.2
IN8 + PhOPh + PhOH	-8.1	-5.3	-10.1	1.7	1.7
IN6 + PhOPh	-10.7	-7.7	1.9	5.5	3.6
TS3 + PhOPh	-9.6	-8.0	2.2	4.9	3.0
IN9 + PhOPh + PhH	-34.9	-31.7	-35.4	-15.7	-15.7
(c) The reductive elimination					
TS5 + PhOPh + PhOH	-5.6	-3.9	-8.2	1.2	1.2
TS6 + PhOPh + PhH	-8.9	-7.4	-12.2	3.7	3.7
IN1 + PhOH +PhH	-21.8	-17.3	-20.0	-20.3	-18.4

Table S2. Relative electronic energies, enthalpies, gas-phase free energies, free energies with solvent correction at 1 atm, and free energies with solvent correction at 1 M (in kcal/mol) for hydrogenation of benzene. The gas phase geometry structures were optimized by B3LYP/BS1. The solvent correction free energies were calculated by M06/BS2 in *m*-xylene.

	Relative Energy (kcal/mol)				
	B3LYP/BS1			M06/BS2	
	ΔE_{elec}	ΔH_{gas}	ΔG_{gas} (1atm)	ΔG_{sol} (1atm)	ΔG_{sol} (1M)
Ni(SIPr)(η^6-C_6H_6) + H_2 + C_6H_6	2.0	2.0	4.0	0.0	0.0
IN10 + H_2 + C_6H_6	0.0	0.0	0.0	0.0	0.0
IN11 + C_6H_6	0.0	1.9	13.1	8.4	6.5
TS7 + C_6H_6	12.8	13.7	26.3	27.0	25.1
IN12 + C_6H_6	12.0	14.7	27.0	26.4	24.5
TS8 + C_6H_6	27.0	28.9	38.6	40.9	39.0
IN13 + C_6H_6	-7.3	-1.2	9.1	5.7	3.8
IN10 + C_6H_8	1.2	6.9	14.8	9.1	7.2